

Deflection angle evolution with plasma medium and without plasma medium in a parameterized black hole

Xiaoling He,^{1,*} Tianyu Xu,^{1,†} Yun Yu,^{2,‡} Anosha Karamat,^{3,§} Rimsha Babar,^{4,¶} and Riasat Ali^{5,**}

¹*School of Science, Zhejiang University of Science and Technology, Hangzhou 310023, Zhejiang, China.*

²*Zhejiang University of Science and Technology, Hangzhou 310023, Zhejiang, China*

³*Department of Mathematics, Minhaj University, Lahore-54000, Pakistan*

⁴*Division of Science and Technology, University of Education, Township, Lahore-54590, Pakistan*

⁵*Department of Mathematics, GC University Faisalabad Layyah Campus, Layyah-31200, Pakistan*

(Dated: March 20, 2023)

Using the Keeton and Petters approach, we determine the deflection angle. We also investigate the motion of photons around a parameterized black hole in the presence of non-magnetized cold plasma by using a new ray-tracing algorithm. In spherically symmetric spacetime, we examine the influence of the plasma by applying the Hamiltonian equation on the deflection angle as well as shadow. It is examined to derive the rays analytically from Hamilton's equation by separating the metric and the plasma frequency. We study that the presence of plasma affects the deflection angle as well as shadow for the parameterized black hole and they depend on plasma frequency. If the plasma frequency is significantly lower than the photon frequency, the photon sphere and shadow radius expressions can be linearized around the values found for space light rays. Furthermore, we have graphically analyzed the behavior of shadow for distinct positions under the effects of plasma frequency as well as low density plasma medium.

I. INTRODUCTION

Black holes are invisible objects that are typically thought to arise in the gravitational collapse of enormous astronomical objects, as predicted by Einstein's general relativity (GR). It is commonly known that photons released from a lit source behind a black hole (BH) will create the so-called BH shadow, a two-dimensional dark region in the observer's sky. The BH's shadow, which is an impression of the BH, tells us important things about the BH. For instance, one can determine the BH's charge and spin [1–6] as well as limit certain additional parameters brought about by changing gravities [7–11] from the shadow of the BH. First, Synge [12] and later Lunin [13] looked at the perfect circle-shaped shadow that a spherically symmetric BH casts. They also presented formulas to determine the shadow size and angular radius, respectively. Bardeen [14] was the first to examine the shadow produced by a Kerr BH. Because of the dragging action, the shadow shape is modified. Since then, there has been a lot of research done in the literature on the BH shadow. For instance, [15] looked at the BH shadow and photon sphere in dynamically changing spacetimes.

The gravitational lensing effect is the process by which BHs bend the escaping light beams in addition to capturing them. Gravitational lensing is another effective approach that gives us a vast amount of data on BHs, including their location, angular momentum and mass. The geodesic technique [16–20] has been intensively researched for gravitational lensing for black holes, wormholes, cosmic strings and other phenomena since the first measurement of the deflection angle of light by the sun. Gibbons and Werner presented a different approach in ref. [21] for calculating the weak deflection angle of light by a spherically symmetric BH within the framework of optical geometry using the Gauss-Bonnet theorem and then, Werner [22] extended this method to stationary BHs by applying Kerr-Randers optical metric. Additionally, whereas the impact of plasma on light rays can often be disregarded in astronomical contexts, this is not the case for light rays in the radio frequency spectrum. The effects of the solar corona, which is thought of as a non-magnetized pressureless plasma, on the time delay [23] and deflection angle when the light rays propagate close to the Sun [24] are one well known examples. Later, Perlick studied the impact of a non-homogeneous plasma on a light deflection in the equatorial plane of the Kerr metric and in the Schwarzschild metric [25]. Since

*Electronic address: hxfudan@aliyun.com

†Electronic address: 744549568@qq.com

‡Electronic address: 1957517787@qq.com

§Electronic address: anosha.karamat2@gmail.com

¶Electronic address: rimsha.babar10@gmail.com

**Electronic address: riasatyasin@gmail.com

then, research on how plasma affects light transmission has become increasingly popular. For instance, refs. [26–31] looked at the effects of plasma on gravitational lensing by BHs and compact objects. In refs. [32–35], the shadows of wormholes and BHs surrounded by plasma were studied.

One of the most important reasons to study quantum gravity is the search for ultraviolet complete gravitational theories that could prevent space-time singularity. There are numerous attempts, including string field theory and quantum gravity, even though we do not yet have a fully formed quantum gravity theory. According to a common assumption shared by nearly all of these theories, there should be an intrinsic modified geometry in space-time [36] that is on the order of the Planck length. A configuration with this much extension suggests that space-time is not local [37–40]. So, it is expected that the linear correction to GR is the first-order correction [41–49] of quantum theory. The quantum gravity and shadow are compulsory components to study BH geometry.

The deflection angle for Einstein-Maxwell-Dilaton-Axion like BH using the methodology developed by Gibbons and Werner has been studied [50]. Further evidence that the gravitational lensing effect is a global and even topological phenomenon, i.e., there are several light rays converging between the source and observer, was provided by the fact that the deflection of a light ray was determined outside of the lensing area. The weak limit approach [51] of the Gauss-Bonnet theorem was used to compute the deflection angle of a null aether like BH by investigating the light beams in a BH gravitational field. Matsuno calculated [52] the deflection angles while taking into account photon movements around a charged squashed Kaluza-Klein like BH particle in an unmagnetized homogeneous cold plasma medium. The light deflection angle at the leading order terms was determined using the Gauss-Bonnet theorem and a straight line approach by [53] and also examined the gravitational lensing of the Einstein-Cartan-Kibble-Sciama like BH in the weak field approximation. The Gauss-Bonnet theorem has been used [54] to study weak gravitational lensing in Kerr-Newman-Kasuya like optical spacetime, where optical geometry provides a more geometrical view. It was found that the deflection angle decreased linearly with the additional magnetic charge compared to Kerr-Newman BHs.

In our work, we explore the deflection angle by using the Keeton and Petters technique and ray-tracing algorithm from the photon pathway around a BH in the presence of non-plasma and plasma with radial density and evaluate the impacts of plasma on the BH shadow. We have formulated our paper by the following pattern: In Sec. **II**, we review the BH metric and study the effects of deformation parameter to metric function. In Sec. **III**, using the Keeton and Petters approach, to determine the deflection angle. In Sec. **IV** explains the motion equation of light ray in the scenario of BH with plasma. In Sec. **V**, we study the circular light orbits that are very important for the creation of the shadow. Sec. **VI**, computes the angular radius of the BH shadow. In Sec. **VII**, we graphically discuss the impacts of different parameters on BH Shadow. Sec. **VIII**, examines the case of a low-density plasma Shadow. In Sec. **IX**, we summarize the results.

II. DEFLECTION ANGLE ANALYSIS WITH PLASMA MEDIUM

Huang et al. used [63] a new ray-tracing algorithm to examine the photon's velocity around a BH in the presence of plasma, whose density is a function of the radius coordinate, and look into the impact of the plasma on the BHs shadow. We expect that the spacetime is loaded up with a non-magnetized cold plasma whose electron plasma frequency w_p only seems on the coordinate of radius (r) in the form

$$w_p^2(r) = \frac{4\pi E(r)e^2}{m}, \quad (1)$$

whereas $E(r)$, m and e are the number of electron's density in the non-magnetized plasma, electron mass and electron charge, respectively. This plasma's refraction index i , is influenced by the photon's frequency as measured by a static observer and the radius coordinate r in the following way

$$i^2(r, w) = 1 - \frac{w_p^2(r)}{w^2}. \quad (2)$$

Due to the spherical symmetry, we can limit to the equatorial plane $\theta = \frac{\pi}{2}$, $u_\theta = 0$. The Hamiltonian explains the particle's motion in a pressure-free and non-magnetized plasma as

$$\begin{aligned} H &= \frac{1}{2} (g^{ik} u_i u_k + w_p^2(r)), \\ &= \frac{1}{2} \left(-\frac{u_t^2}{A(r)} + \frac{u_r^2}{B(r)} + \frac{u_\phi^2}{C(r)} + w_p^2(r) \right). \end{aligned} \quad (3)$$

Light waves for Hamilton equations imply that

$$\dot{u}_i = -\frac{\partial H}{\partial \delta^i}, \quad \delta^i = \frac{\partial H}{\partial u_i}, \quad (4)$$

it can be written as

$$\dot{u}_t = -\frac{\partial H}{\partial t} = 0, \quad (5)$$

$$\dot{u}_\phi = -\frac{\partial H}{\partial \phi} = 0, \quad (6)$$

$$\dot{u}_r = -\frac{\partial H}{\partial r} = \frac{1}{2} \left(-\frac{u_t^2 \dot{A}(r)}{A^2(r)} + \frac{u_r^2 \dot{B}(r)}{B^2(r)} + \frac{s_\phi^2 \dot{C}(r)}{C^2(r)} - \frac{d}{dr} w_p^2(r) \right), \quad (7)$$

$$\dot{t} = \frac{\partial H}{\partial u_t} = -\frac{u_t}{A(r)}, \quad (8)$$

$$\dot{r} = \frac{\partial H}{\partial u_r} = \frac{u_r}{B(r)}, \quad (9)$$

$$\dot{\phi} = \frac{\partial H}{\partial u_\phi} = \frac{u_\phi}{C(r)}, \quad (10)$$

for $H = 0$, we have

$$0 = -\frac{u_t^2}{A(r)} + \frac{u_r^2}{B(r)} + \frac{u_\phi^2}{C(r)} + w_p^2(r), \quad (11)$$

here, dot and prime shows differentiation w. r. t an affine parameter and r , respectively. It follows from Eq. (5) and (6) that u_t and u_ϕ represents constants of motion. We may type $w_0 = -u_t$. In case of a asymptotically flat spacetime, the w_0 is fixed and $A(r) \rightarrow 1$ as $r \rightarrow \infty$ and the frequency of a static observer represented by $w(r)$ can be defined by redshift formula as

$$w(r) = \frac{w_0}{\sqrt{A(r)}}. \quad (12)$$

From the equation (11), the constant motion w_0 of light beam is specified to the particular region with

$$\frac{w_0^2}{A(r)} > w_p^2(r). \quad (13)$$

The photons frequency at that place should be greater than the plasma frequency, according to Eq. (13). It is true for the light transmission in a medium of plasma. We consider Eqs. (9) and (10), to get the equation of orbit

$$\frac{dr}{d\phi} = \frac{\dot{r}}{\dot{\phi}} = \frac{C(r)u_r}{B(r)u_\phi}. \quad (14)$$

By substituting for u_r from equation (11), which is taken by

$$\frac{dr}{d\phi} = \pm \frac{\sqrt{C(r)}}{\sqrt{B(r)}} \left(\sqrt{\frac{w_0^2}{u_\phi^2} D(r)^2 - 1} \right), \quad (15)$$

with

$$\frac{w_0^2}{u_\phi^2} D(r)^2 - 1 > 0, \quad D^2(r) = \frac{C(r)}{A(r)} \left(1 - A(r) \frac{w_p^2(r)}{w_0^2} \right). \quad (16)$$

In this case, the equation (15) sign-in must be suitably followed and the orbit should be divided into segments at the points r is slowly decreasing and increasing in connection to ϕ . The expression for the deflection angle (Ψ) for an infinite light beam with a radius of Y and an additional infinity is produced by integrating over the orbit, we get

$$\pi + \Psi = 2 \int_Y^\infty \frac{\sqrt{B(r)}}{\sqrt{C(r)}} \left(\frac{w_0^2}{u_\phi^2} D^2(r) - 1 \right)^{-\frac{1}{2}} dr. \quad (17)$$

Since Y is related with the pivot of trajectory, the specified case $\frac{dr}{d\phi}|_Y = 0$ must be fulfilled. The above mentioned equation determines the following relationship between the radius Y and the constant motion $\frac{u_\phi}{w_0}$ as follows

$$D^2(X) = \frac{u_\phi^2}{w_0^2}. \quad (18)$$

In terms of w and Y , the angle of deflection for a certain plasma distribution can be expressed as follows

$$\pi + \Psi = 2 \int_Y^\infty \left(\frac{\frac{r^5}{r^3 - \eta - 2Mr^2} - \frac{r^2 w_p^2(r)}{w_0^2}}{\frac{Y^5}{Y^3 - \eta - 2MY^2} - \frac{Y^2 w_p^2(Y)}{w_0^2}} - 1 \right)^{-\frac{1}{2}} \frac{dr}{\sqrt{r^3 - \eta - 2Mr^2}}. \quad (19)$$

The deflection angle is dependent by the horizon radius, the infinite radius of the light wave Y , the BH mass, the photon and plasma frequency, the BH geometry, and BH deformation parameter. When $\eta = 0$, the equation (19) for the plasma's deflection angle on Schwarzschild spacetime was developed in [64]. In [65], it was derived using Synge's method and formulated in terms of an elliptic integral for a homogeneous plasma. Further, the strong deflection limit $\Psi \gg 1$ was examined. Moreover, we conclude that for $\eta = 0$, we recover the deflection angle for Schwarzschild BH as calculated in [33].

III. ORBITS OF LIGHT

For photons emitted from the observer's screen in the previous ray-tracing method, there are only two possible final states: either the photon has been absorbed by the BH or it is scattered indefinitely. Once released, the photons will gradually scatter around the BH, which is where the shadow of a BH is situated in the observer's image plane. This section will discuss the condition of circular light orbits, which is necessary for locating the shadow. It is important to note that the light is flowing in a circular direction while the states $\dot{r} = 0$ and $\ddot{r} = 0$. Eqs. (9) and (11) with $u_r = 0$ give us the relation shown below:

$$0 = -\frac{w_0^2}{A(r)} + \frac{u_\phi^2}{C(r)} + w_p^2(r). \quad (20)$$

As an approach, (9) implies

$$\dot{u}_r = \frac{d}{d\lambda}(B(r)\dot{r}) = \ddot{r}B(r) + \dot{r}^2 B'(r). \quad (21)$$

If $\dot{r} = 0$, $\ddot{r} = 0$ and $\dot{u}_r = 0$, then Eq. (6) represents the light orbits second equation

$$0 = -\frac{w_0^2 A'(r)}{A^2(r)} + \frac{u_\phi^2 C'(r)}{C^2(r)} - \frac{d}{dr} w_p^2(r). \quad (22)$$

For u_ϕ^2 , we can compute the solution from Eqs. (20) and (22) as

$$u_\phi^2 = C(r) \left(\frac{w_0^2}{A(r)} - w_p^2(r) \right), \quad (23)$$

$$u_\phi^2 = \frac{C^2(r)}{C'(r)} \left(\frac{w_0^2 A'(r)}{A^2(r)} + \frac{d}{dr} w_p^2(r) \right). \quad (24)$$

By eliminating these two equations from one another after making a few straightforward adjustments provides the following result for the radius of a circular light orbit in the form

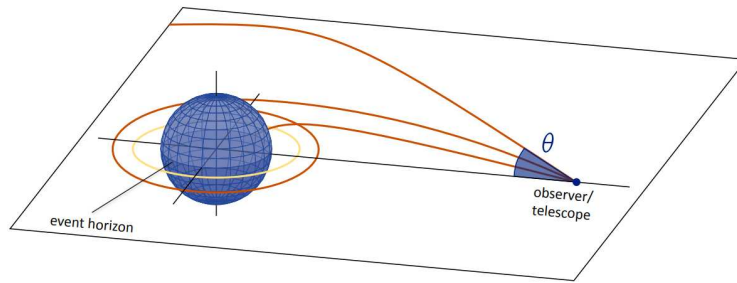
$$0 = r^2 \left(5r^3 - 5\eta - 10r^2 M - 3r^3 + 4r^6 M \right) - \left(r^3 - \eta - 2r^2 M \right)^2 \left[\frac{2w_p^2(r)}{w_0^2} - \frac{r^2}{w_0^2} \frac{d}{dr} w_p^2(r) \right], \quad (25)$$

at which the property $D^2(r)$ is produced by the formula (16). The photon sphere radius can be calculated by using the (25) solution for $r = r_p$. A light moving tangentially into a sphere always goes in a circle with radius $r = r_p$. The furthest photon circle is consistently unstable in terms of radial disorder if the BH space-time is asymptotically

flat with $w_p \rightarrow A \ 0$ and $r \rightarrow \infty$. This implies that the asymptotic light beams that reach them could act as limit curves for the circular photon's orbits. The exterior photon circle's radius and the analytical point of the recently discussed un-important radius X are identical. A light ray goes to its point of origin when it leaves its infinity-based origin and goes to a minimum radius Y that is higher than r_p . A light beam spirals asymptotically along the direction of a photon sphere's circular orbit in the case where $Y = r_p$. The fact that the equation (25) can be reduced to the Atkinson scenario [66] for $w_p(r) = 0$ is crucial.

IV. SHADOW RADIUS

The shadow is a visualization of a spherically symmetric space-time. By taking into account the description of the expression from the preceding section, we examine the effects of plasma on an incident light. We discuss the two classifications of these incident photons. Through the BH, photons of first-class light are reflected back and move continuously. The photon of second-class light is going toward the BH's horizon.



Let's start by supposing that there isn't a source of light in the observer's sky that would interfere with the BH-observer relationship. The BH's shadow is represented by the sphere in the observer's sky. The starting trajectory of the photon's light, which is asymptotically radial in the direction of the outer photon sphere, determines the shadow radius.

$$\cot \Phi = \frac{g_{rr}}{g_{\phi\phi}} \frac{dr}{d\phi} \Big|_{r=r_0} = \frac{\sqrt{B(r)}}{\sqrt{C(r)}} \frac{dr}{d\phi} \Big|_{r=r_0}. \quad (26)$$

Using the equation (18) to the orbit equation (15), we obtain the minimum \hat{A} ray of light as it approaches a minimal radius Y .

$$\frac{dr}{d\phi} = \pm \frac{\sqrt{C(r)}}{\sqrt{B(r)}} \sqrt{\frac{D^2(r)}{D^2(X)} - 1}. \quad (27)$$

For the angle Φ , we obtain the following:

$$\cot^2 \Phi = \frac{D^2(r_0)}{D^2(X)} - 1. \quad (28)$$

This suggests

$$\sin^2 \Phi = \frac{D^2(r_0)}{D^2(X)}. \quad (29)$$

The limit of shadows is determined by the approximate rotation of light into a sphere with a radius of r_p . As a result, sending $X \rightarrow r_p$ gives the angular shadow size in Eq. (29) as

$$\sin^2 \Phi = \frac{D^2(r_{ph})}{D^2(r_0)}, \quad (30)$$

where the equation expression (16) expresses $D(r)$. We can assume that the observer is situated in a zone of low-density plasma. The equation result (16) gives

$$D^2(r_0) = \frac{C(r_0)}{A(r_0)}, \quad (31)$$

and equation (30) implies

$$\sin^2 \Phi = \frac{r_{ph}^5 (r_0^3 - \eta - 2Mr_0^2)}{r_0^5 (r_{ph}^3 - \eta - 2Mr_{ph}^2)} \left[1 - \left(1 - \frac{\eta}{r_{ph}^3} - \frac{2M}{r_{ph}} \right) \frac{\omega_p^2(r_{ph})}{\omega_0^2} \right]. \quad (32)$$

This demonstrates how the plasma is gradually affecting the shadow's decreasing radius. It seems to be the case for all spherically symmetric spacetimes, such as wormhole metrics and compact metrics with an instability photon sphere. These objects would cast shadows like BHs if the light were not shining from the direction of the centre object towards the observer. In order for the light rays in the photon sphere to function as limit curves, it is absolutely necessary for them to be unstable in relation to radial perturbations. Because of this, the shadow can be constructed in any static, spherically symmetric spacetime that accepts an unstable photon sphere. This includes black holes as well as wormholes. The outermost photon sphere is always unstable in a static, asymptotically flat, spherically symmetric spacetime, provided that the plasma density tends to zero for $r \rightarrow \infty$. It is also worth mentioning here that for $\eta = 0$ and $r_{ph} = 3M$ in Eq. (32), we recover the radius of shadow for Schwarzschild BH [33].

V. GRAPHICAL ANALYSIS FOR SHADOW OF BLACK HOLE

This section gives the graphical behavior for shadow of parameterized BH.

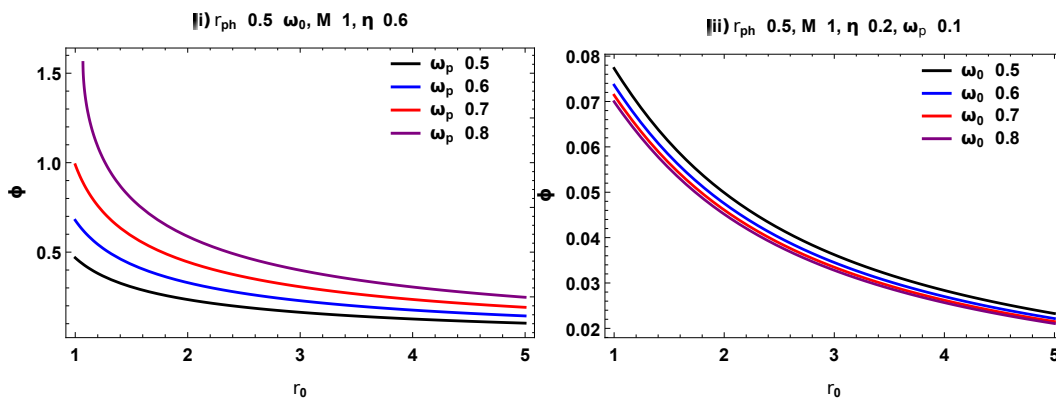


Figure 2: The BH shadow Φ versus radius r_0 for various ω_p , ω_0 and fixed $r_{ph} = 0.5 = \omega_0$, $M = 1$ and $\eta = 0.6$ in the left plot while for fixed $r_{ph} = 0.5$, $\omega_0 = 0.1$, $M = 1$ and $\eta = 0.2$ in the right plot.

The left plot of **Fig. 2** shows the behavior of the angular radius of shadow with static observer at distinct positions r_0 for varying ω_p . The Φ slowly decreases and then, it gets a flat form for rising r_0 . It is notable that the Φ rises for rising values of ω_p .

In the right plot of **Fig. 2**, the Φ represents the behavior with r_0 for changing values of ω_0 . The Φ slowly decreases till $r_0 \rightarrow \infty$. The Φ decreases with rising ω_0 .

From **Fig. 2**, we conclude that the BH shadow is smaller for different variations of r_0 . To get large shadow radius in strong gravity, the frequency parameter must be extremely small.

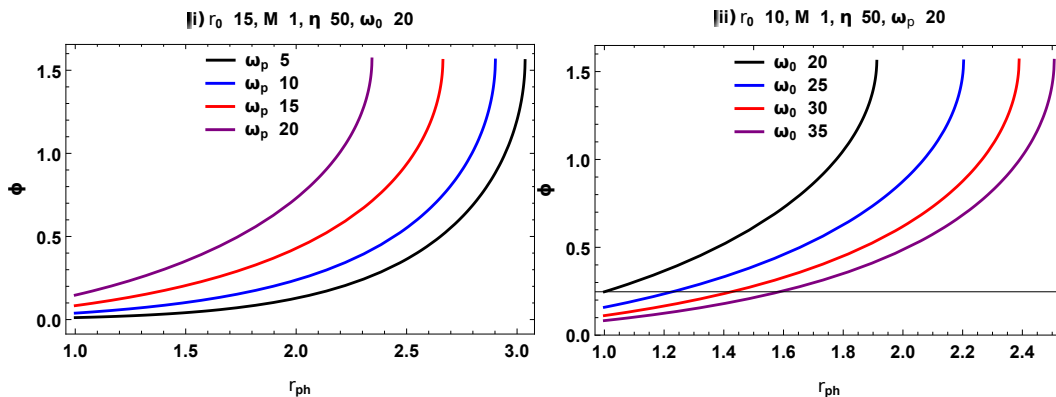


Figure 3: The BH shadow angular radius w.r.t r_{ph} for various ω_p , ω_0 and fixed $M = 1$, $\eta = 50$, $\omega_0 = 20$.

The left plot in **Fig. 3** represents the dependency of Φ versus r_{ph} for different values of ω_p . In the left plot, the Φ continuously goes on increasing. The Φ reduces for rising values of ω_p . In the right plot of **Fig. 3**, the Φ shows a rising attitude for rising r_{ph} as well as the radius of shadow increase for rising values of ω_0 .

The **Fig. 3** demonstrates that the BH shadow is smaller for different variations of r_{ph} but it shows an increasing behavior. To get large shadow radius in strong gravity, the frequency parameter must be extremely small.

VI. A LOW DENSITY PLASMA'S SHADOW

If the plasma frequency is significantly lower than the photon frequency, the photon sphere and shadow radius expressions can be linearized around the values found for space light rays. This is addressed by modifying equation (16) as

$$D^2(r) = Z(r)(1 - \varsigma\alpha(r)), \quad (33)$$

whereas

$$Z(r) = \frac{C(r)}{A(r)}, \quad \alpha(r) = \frac{A(r)w_p^2(r)}{w_0^2} = \frac{w_p^2(r)}{w^2(r)}. \quad (34)$$

We include an accounts parameter ς , which is set to unity once all results have been linearized. This consequence of linearity can be deduced by power law i.e., $\frac{w_p^2(r)}{w^2(r)} = \beta_0 \frac{M^k}{r^k}$, where $\beta_0 > 0$ and $k \geq 0$ that represents dimensionless constants. A detailed example for Schwarzschild black hole for this consequence is given in [67]. Now, the photon sphere result (25) written as

$$0 = Z'(r)(1 - \varsigma\alpha(r)) - \varsigma Z(r)\alpha'(r). \quad (35)$$

It is possible to express the equation's solution as follows

$$r_{ph} = r_{ph}^0 + \varsigma r_{ph}^1 + \dots, \quad (36)$$

in the absence of plasma with a solution r_{ph}^0 such that

$$Z'(r_{ph}^0) = 0. \quad (37)$$

We derive the ς coefficients by inserting these formulas into (35) and after comparing them, we get

$$r_{ph}^1 = \frac{Z(r_{ph}^0)\alpha'(r_{ph}^0)}{Z''(r_{ph}^0)}. \quad (38)$$

In relation to the values of $\alpha'(r_{ph}^0)$ and $Z''(r_{ph}^0)$, this equation can be either positive or negative, so that the plasma can move the light sphere outside or inside. Now, we implement an expansion (36) to the shadow result (30). Once more set all components equal to unity while ignoring any quadratic and higher order factors, we obtain

$$\sin^2 \Phi = \frac{\tilde{r}^5(r_0^3 - \eta - 2r_0^2 M)}{r_0^5(\tilde{r}^3 - \eta - 2\tilde{r}^2 M)} \left[1 - \left(1 - \frac{\eta}{\tilde{r}^3} - \frac{2M}{\tilde{r}} \right) \frac{w_p^2(\tilde{r})}{w_0^2} + \left(1 - \frac{\eta}{r_0^3} - \frac{2M}{r_0} \right) \frac{w_p^2(r_0)}{w_0^2} \right], \quad (39)$$

with $\tilde{r} = r_{ph}^0$. Note that the computation for to within this order no longer takes r_{ph}^1 into account. From the Eq. (39), the plasma has less of an impact on the shadow than $(1 - \frac{\eta}{r_0^3} - \frac{2M}{r_0}) \frac{w_p^2(r_0)}{w_0^2} < (1 - \frac{\eta}{\tilde{r}^3} - \frac{2M}{\tilde{r}}) \frac{w_p^2(\tilde{r})}{w_0^2}$. The photon sphere radius r_{ph} must be computed for a given metric (??), a defined photon frequency at infinity w_0 , and a specified plasma frequency that satisfies the case $w_p(r) \ll w(r)$. Approximate r_{ph}^0 from (37) and r_{ph}^1 from (38), then estimate r_{ph} allowing to (38) with $\varsigma = 1$. Then, write down the functions $Z(r)$ and $\alpha(r)$ (see (34)). In this procedure, we have to put r_{ph}^0 into the expression to obtain the radius of shadow angular Φ for observer particular r_0 position (39).

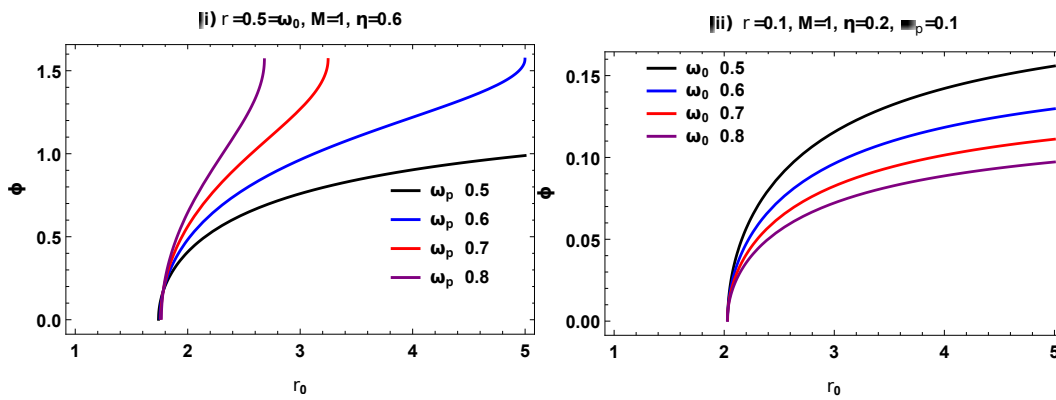


Figure 4: The plasma shadow Φ versus radius r_0 for various ω_p , ω_0 and fixed $\tilde{r} = 0.5 = \omega_0$, $M = 1$ and $\eta = 0.6$ in the left plot while for fixed $\tilde{r} = 0.1 = \omega_0$, $M = 1$ and $\eta = 0.2$ in the right plot.

The left plot of **Fig. 4** shows the behavior of the angular radius of shadow with static observer at distinct positions r_0 for varying ω_p in low density medium. The Φ continuously goes on increasing but the radius of shadow becomes smaller. The plasma shadow rises for rising values of ω_p . In the right plot of **Fig. 4**, the Φ exponentially rises for rising r_0 . It is also observable that the shadow radius in low density plasma is smaller as compared to **Fig. 3**. The **Fig. 4** states that the BH shadow goes on increasing for different variations of distinct observer r_0 . To get a very large shadow radius in strong gravity, the frequency parameter must be extremely small.

VII. CONCLUSIONS

In this research, we have examined deformation parameter effect on metric function by considering the methodology of Keeton and Petters and the framework of \tilde{A} PPN \tilde{A} is a direct way for dealing with all types of gravity theories in which the weak-deflection limit is stated as a series expansion with \tilde{A} single variable M . The deflection angle depends on the deformation parameter (η), the impact parameter (b) and the mass (M). The results we have obtained for BH solutions in the presence of non-plasma mediums show that deflection angle has a direct relationship with mass M and a parameter η , indicating that BH with greater mass has greater gravitational pull and bends the light passing by it at large angles. While BH with smaller mass deflect the light at a smaller angle. Additionally, we observe that deflection angle has an inverse relationship with impact parameter b , demonstrating that a smaller value of the impact parameter results in a larger deflection angle and vice versa. Moreover, we conclude that for $\eta = 0$, we recover the deflection angle for Schwarzschild BH.

We have examined the BH shadow radius in plasma as well as low density plasma medium by using the Hamilton equation to describe photon motion. To do so, by using a new ray-tracing algorithm, we numerically solved the Hamilton equations to determine the BH shadow radius. The size and shape of the BH shadow can alter when there is plasma surrounding a BH because the trajectory of a photon is dependent on the photon frequency. The photon-absorbing and scattering actions of plasma electrons are not taken into consideration. Further, we ignore the plasma particle's gravitational field. Furthermore, the size of shadow always shrinks when plasma is present and for $\eta = 0$ and $r_{ph} = 3M$ in Eq. (32), we get the radius of shadow for Schwarzschild BH. At low frequency plasma density, the shadow of a BH is shown to appear on the observer's screen. The BH shadow is identical to that BH at high frequency, and the influence of the plasma is minimal. Furthermore, the presence of a plasma may result in the formation of a number of structures in the BH image.

Moreover, we have graphically analyzed the behavior of shadow for distinct positions under the effects of plasma frequency ω_p and ω_0 in plasma as well as low density plasma medium. We have observed that Φ slowly decreases and then, it gets a flat form for rising r_0 . It is notable that the Φ rises for rising values of ω_p . For changing values of ω_0 , the Φ slowly decreases till $r_0 \rightarrow \infty$. The Φ decreases with rising ω_0 . The BH shadow is smaller for different variations of r_0 . To get large shadow radius in strong gravity, the frequency parameter must be extremely small. The Φ reduces for rising values of ω_p in the region $1 \leq r_{ph} \leq 5$. It shows a rising attitude for rising r_{ph} as well as the radius of shadow increases for rising values of ω_0 . In low density medium, the Φ continuously goes on increasing but the radius of shadow becomes smaller. The plasma shadow rises for rising values of ω_p . The Φ exponentially rises for rising r_0 for varying ω_0 . It is also observable that the shadow radius in low density plasma is smaller as compared to **Fig. 3**. The BH shadow is goes on increasing for different variations of distinct observer r_0 . To get a very large shadow radius in strong gravity, the frequency parameter must be extremely small. We have simply taken into account the photon motion in a stationary, non-magnetized, pressure-free plasma in the background of a BH here as a first step towards

understanding the influence of ionised matter on the various astrophysical compact objects. Future research should naturally build on these findings to incorporate more complex yet realistic plasma models.

We anticipate that the observation will provide us with important hints and surprises regarding space-time and the distribution of matter in the vicinity of the BH, as revealed by the future results of the Event Horizon Telescope (EHT). However, expecting that EHT can effectively limit the plasma density distribution's properties is suggested. Although the pulling effect extends the shadow of a revolving BH in this position.

-
- [1] R. Takahashi, It Shapes and positions of black hole shadows in accretion disks and spin parameters of black holes. *Astrophys. J.* **611**(2004)996.
 - [2] N. Tsukamoto, Z.L. Li, C. Bambi, Constraining the spin and the deformation parameters from the black hole shadow. *JCAP* **1406**(2014)043.
 - [3] A.F. Zakharov, F.D. Paolis, G. Ingrosso, A.A. Nucita, Measuring the black hole parameters in the galactic center with RADIOASTRON. *New Astron.* **10**(2005)479.
 - [4] K. Hioki, K. Maeda, Measurement of the Kerr spin parameter by observation of a compact object's shadow. *Phys. Rev. D* **80**(2009)024042.
 - [5] A.F. Zakharov, Constraints on a charge in the Reissner-Nordstrom metric for the black hole at the Galactic Center. *Phys. Rev. D* **90**(2014)062007.
 - [6] Z.L. Li, C. Bambi, Measuring the Kerr spin parameter of regular black holes from their shadow. *JCAP* **1401**(2014)041.
 - [7] J.C.S. Neves, Constraining the tidal charge of brane black holes using their shadows. *Eur. Phys. J. C* **80**(2020)717.
 - [8] L. Amarilla, E.F. Eiroa, G. Giribet, Null geodesics and shadow of a rotating black hole in extended Chern-Simons modified gravity. *Phys. Rev. D* **81**(2010)124045.
 - [9] J.W. Moffat, Modified Gravity Black Holes and their Observable Shadows. *Eur. Phys. J. C* **75**(2015)130.
 - [10] L. Amarilla, E.F. Eiroa, Shadow of a rotating braneworld black hole. *Phys. Rev. D* **85**(2012)064019.
 - [11] L. Amarilla, E.F. Eiroa, Shadow of a Kaluza-Klein rotating dilaton black hole. *Phys. Rev. D* **87**(2013)044057.
 - [12] J.L. Synge, The escape of photons from gravitationally intense stars. *Mon. Not. Roy. Astron. Soc.* **131**(1966)463.
 - [13] J.P. Luminet, Image of a spherical black hole with thin accretion disk. *Astron. Astrophys.* **75**(1979)228.
 - [14] J.M. Bardeen, Timelike and Null Geodesics of the Kerr Metric; Gordon and Breach: New York, NY, USA, 1973.
 - [15] A.K. Mishra, S. Chakraborty, S. Sarkar, Understanding photon sphere and black hole shadow in dynamically evolving spacetimes. *Phys. Rev. D* **99**(2019)104080.
 - [16] K.S. Virbhadra, G.F.R. Ellis, Schwarzschild black hole lensing. *Phys. Rev. D* **62**(2000)084003.
 - [17] K.S. Virbhadra, G.F.R. Ellis, Gravitational lensing by naked singularities. *Phys. Rev. D* **65**(2002)103004.
 - [18] V. Bozza, Gravitational lensing in the strong field limit. *Phys. Rev. D* **66**(2002)103001.
 - [19] V. Perlick, On the Exact gravitational lens equation in spherically symmetric and static space-times. *Phys. Rev. D* **69**(2004)064017.
 - [20] C.H. Nam, Implications for the hierarchy problem, inflation and geodesic motion from fiber fabric of spacetime. *Eur. Phys. J. C* **81**(2021)1102.
 - [21] G.W. Gibbons, M.C. Werner, Applications of the Gauss-Bonnet theorem to gravitational lensing. *Class. Quant. Grav.* **25**(2008)235009.
 - [22] M.C. Werner, Gravitational lensing in the Kerr-Randers optical geometry. *Gen. Relativ. Gravit.* **44**(2012)3047.
 - [23] D.O. Muhleman, I.D. Johnston, Radio propagation in the solar gravitational field. *Phys. Rev. Lett.* **17**(1966)455.
 - [24] D.O. Muhleman, R.D. Ekers, E.B. Fomalont, Radio interferometric test of the general relativistic light bending near the sun. *Phys. Rev. Lett.* **24**(1970)1377.
 - [25] V. Perlick, *Ray Optics, Fermat's Principle, and Applications to General Relativity*; Springer: Berlin, Germany, 2000.
 - [26] G.S. Bisnovatyi-Kogan, O.Y. Tsupko, Gravitational lensing in a non-uniform plasma. *Mon. Not. Roy. Astron. Soc.* **404**(2010)1790.
 - [27] A. Rogers, Frequency-dependent effects of gravitational lensing within plasma. *Mon. Not. Roy. Astron. Soc.* **451**(2015)17.
 - [28] V. Morozova, B. Ahmedov, A. Tursunov, Gravitational lensing by a rotating massive object in a plasma. *Astrophys. Space Sci.* **346**(2013)513.
 - [29] C.A. Benavides-Gallego, A.A. Abdujabbarov, C. Bambi, Gravitational lensing for a boosted Kerr black hole in the presence of plasma. *Eur. Phys. J. C* **78**(2018)694.
 - [30] G. Crisnejo, E. Gallo, Weak lensing in a plasma medium and gravitational deflection of massive particles using the Gauss-Bonnet theorem. A unified treatment. *Phys. Rev. D* **97**(2018)124016.
 - [31] G. Bisnovatyi-Kogan, O. Tsupko, Gravitational Lensing in Presence of Plasma: Strong Lens Systems, Black Hole Lensing and Shadow. *Universe* **3**(2017)57.
 - [32] F. Atamurotov, B. Ahmedov, Optical properties of black hole in the presence of plasma: Shadow. *Phys. Rev. D* **92**(2015)084005.
 - [33] V. Perlick, O.Y. Tsupko, G.S. Bisnovatyi-Kogan, Influence of a plasma on the shadow of a spherically symmetric black hole. *Phys. Rev. D* **92**(2015)104031.
 - [34] V. Perlick, O.Y. Tsupko, Light propagation in a plasma on Kerr spacetime: Separation of the Hamilton-Jacobi equation and calculation of the shadow. *Phys. Rev. D* **95**(2017)104003.

- [35] H.P. Yan, Influence of a plasma on the observational signature of a high-spin Kerr black hole. *Phys. Rev. D* **99**(2019)084050.
- [36] S. Das, E.C. Vagenas, Universality of Quantum Gravity Corrections. *Phys. Rev. Lett.* **101**(2008)221301.
- [37] S. Masood, M. Faizal, Z. Zaz, A.F. Ali, J. Raza, M.B. Shah, The most general form of deformation of the Heisenberg algebra from the generalized uncertainty principle. *Phys. Lett. B* **763**(2016)218.
- [38] L. Modesto, I.L. Shapiro, Superrenormalizable quantum gravity with complex ghosts. *Phys. Lett. B* **755**(2016)279.
- [39] L. Modesto, Super-renormalizable or finite Lee-Wick quantum gravity. *Nucl. Phys. B* **909**(2016)584.
- [40] M. Faizal, A.F. Ali, A. Nassar, Generalized uncertainty principle as a consequence of the effective field theory. *Phys. Lett. B* **765**(2017)238.
- [41] R. Ali, R. Babar, M. Asgher, S. A. A. Shah, Evaporation of black hole under the effect of quantum gravity. *Int. J. Geom. Methods Mod. Phys.* **19**(2022)2250017.
- [42] R. Ali, K. Bamba, S. A. A. Shah, Effect of quantum gravity on the stability of black holes. *Symmetry* **631**(2019)11.
- [43] R. Ali, M. Asgher, M.F. Malik, Gravitational analysis of neutral regular black hole in Rastall gravity. *Mod. Phys. Lett. A* **35**(2020) 2050225.
- [44] R. Ali, K. Bamba, M. Asgher, S. A. A. Shah, Tunneling under the influence of quantum gravity in black rings. *Int. J. Mod. Phys. D* **30**(2021)2150002.
- [45] R. Ali, R. Babar, M. Asgher, S. A. A. Shah, Gravity effects on Hawking radiation from charged black strings in Rastall theory. *Annals of Physics*, **432**(2021)168572.
- [46] R. Ali, M. Asgher, Tunneling Analysis Under the Influences of Einstein-Gauss-Bonnet Black Holes Gravity Theory. *New Astronomy* **93**(2022)101759.
- [47] R. Babar, M. Asgher, R. Ali, Gravitational analysis of Einstein-non-linear-Maxwell-Yukawa black hole under the effect of Newman-Janis algorithm. *Phys. Scr.* **97**(2022)125201.
- [48] R. Ali, R. Babar, P.K. Sahoo, Quantum gravity evolution in the Hawking radiation of a rotating regular Hayward black hole. *Physics of the Dark Universe* **35**(2022)100948.
- [49] R. Ali, R. Babar, M. Asgher, Gravitational Analysis of Rotating Charged Black-Hole-Like Solution in Einstein's Gauss Bonnet Gravity. *Annalen der Physik* **2200074**(2022)12.
- [50] W. Javed, R. Babar, A. Övgün, Effect of the dilaton field and plasma medium on deflection angle by black holes in Einstein-Maxwell-dilaton-axion theory. *Phys. Rev. D* **100**(2019)104032.
- [51] A. Övgün, I. Sakalli, J. Saavedra, Effect of null aether field on weak deflection angle of black holes. *Chinese Phys. C* **44**(2020)125105.
- [52] K. Matsuno, Light deflection by squashed Kaluza-Klein black holes in a plasma medium. *Phys. Rev. D* **103**(2021)044008.
- [53] A. Övgün, I. Sakalli, Testing generalized Einstein Cartan Kibble Sciama gravity using weak deflection angle and shadow cast. *Class. Quantum Grav.* **37**(2020)225003.
- [54] A. Övgün, I. Sakalli, J. Saavedra, Shadow cast and Deflection angle of Kerr-Newman-Kasuya spacetime. *JCAP* **10**(2018)041.
- [55] R. Konoplya, A. Zhidenko, Detection of gravitational waves from black holes: is there a window for alternative theories? *Phys. Lett. B* **756**(2016)350.
- [56] R. B. Magalhaes, L. C. S. Leite, L. C. B. Crispino, Absorption by deformed black holes. *Phys. Lett. B* **805**(2020)135418.
- [57] F. Long, S. Chen, S. Wang, J. Jing, Energy extraction from a Konoplya-Zhidenko rotating non-Kerr black hole. *Nucl. Phys. B* **926**(2018)83.
- [58] R. B. Magalhaes, L. C. S. Leite, L. C. B. Crispino, Parametrized black holes: scattering investigation. *Eur. Phys. J. C* **82**(2022)698.
- [59] C. R. Keeton, A. Petters, Formalism for testing theories of gravity using lensing by compact objects: Static, spherically symmetric case. *Phys. Rev. D* **72**(2005)104006.
- [60] C.R. Keeton, A. Petters, Formalism for testing theories of gravity using lensing by compact objects. II. Probing post-post Newtonian metrics. *Phys. Rev. D* **73**(2006)044024
- [61] W. Javed, H. Irshad, R. C. Pantig, A. Övgün, Weak Deflection Angle by Kalbe Ramond Traversable Wormhole in Plasma and Dark Matter Mediums. *Universe* **8**(2022)599.
- [62] W. Javed, S. Riaz, R. C. Pantig, A. Övgün, Weak gravitational lensing in dark matter and plasma mediums for wormhole-like static aether solution. *Eur. Phys. J. C* **82**(2022)1057.
- [63] Y. Huang, Y. P. Dong, D. J. Liu, Revisiting the shadow of a black hole in the presence of a plasma. *Int. J. Mod. Phys. D* **27**(2018)1850114.
- [64] V. Perlick, *Ray Optics, Fermata's Principle, and Applications to General Relativity* (Springer, Berlin, 2000).
- [65] O. Yu. Tsupko and G. S. Bisnovaty-Kogan, Gravitational lensing in plasma: Relativistic images at homogeneous plasma. *Phys. Rev. D* **87**(2013)124009.
- [66] R. d E. Atkinson, On light tracks near a very massive star, *Astron. J.* **70**(1965)517.
- [67] S. Gennady, B. Kogan, O. Yu. Tsupko, Gravitational Lensing in Presence of Plasma: Strong Lens Systems, Black Hole Lensing and Shadow. *Universe* **3**(2017)57.